Terahertz Transmission Through Patterened Vanadium Oxide Thin Films on Dielectric Substrates

M. Akkaya[1], Y. Demirhan[2], H. Yuce[2], G. Aygun[2], L. Ozyuzer[2], C. Sabah[3] and H. Altan[1]

[1]Department of Physics, Middle East Technical University, 06800, Çankaya Ankara, Turkey
[2]Department of Physics, Izmir Institute of Technology, 35430, Urla, Izmir, Turkey
[3]Department of Electrical and Electronics Engineering, Middle East Technical University- Northern Cyprus Campus (METU-NCC), 99738, Kalkanlı, Güzelyurt, TRNC / Mersin 10, Turkey

Abstract: Patterned and unpatterned films of vanadium oxide grown on dielectric substrates such as fused silica and sapphire were grown and analysed by varying the temperature using terahertz time domain spectroscopy. After investigating the critical transition temperature near 340K, a well-known cross-shaped pattern was studied to observe any resonances upon transmission. Due to the poor conductivity of the films the frequency selective nature of the structure was not observed, however an etalon effect could be seen in the sapphire substrate as opposed to the fused silica substrate above the critical temperature. Dependence of the refractive index difference between substrates upon transmission of the THz pulse is likely in explaining this observed difference.

1 INTRODUCTION

In the electromagnetic (EM) spectrum, the region between Microwave and Infrared Region corresponds to Terahertz (THz) frequency range (Zhang, 2010). This range corresponds to 10^{12} hertz in the spectrum. Generally, this radiation is called T-rays. T-rays have 4.1 meV energy at 1 THz, an equivalent temperature of 48 K, period of 1 ps, wavelength of 300 μm and a corresponding wave number of 33.3 cm^{-1} (Lee, 2009). THz region has a variety of advantages since it falls within reach of both electronics and optics. Therefore, in THz region both technologies are important to generate or to detect THz radiation. Development of time domain terahertz spectroscopic techniques is one of the most successful of THz applications. By using terahertz time domain spectroscopy (THz-TDS), scientists have been able to successfully characterize dielectrics, semiconductors and also superconductors (Grischkowsky, 1990).

It is important to create technologies which can both control the frequency and amplitude or intensity of the radiation in this region. Due to the low energy of these photons it has been a challenge to create devices which work in this frequency range

at room temperature. Metamaterials or frequency selective surfaces offer a method to control the transmission or reflection of terahertz waves in and around the frequency region of interest (Holloway, 2005). Since terahertz radiation is highly reflected by conducting materials recent efforts have concentrated on developing smart materials which can change their conductivity upon a change in a parameter which can be controlled externally. Typically this externally controlled parameter can either be temperature, applied bias or current. Studies have been done with semi and superconducting metasurfaces (Chen, 2006). While superconducting metamaterials have been shown to change the transmission or reflection of terahertz radiation significantly in a narrow bandwidth their commercial use is complicated by the cooling requirements and the power necessary to drive these systems. A device that can show efficient tunability over a broad or narrow bandwidth that operates near room temperature has yet to be demonstrated. Development of smart materials which exhibit a phase transition at or near room temperature will provide the necessary solution to this problem. Offering similar behavior under external control, few studies have been done on room temperature insulators such as Vanadium Oxide (VO_2) which

shows metallic behavior at high temperatures (Jepsen, 2006).

Vanadium dioxide's (VO_2) conductivity is of particular interest since its conductivity changes when the temperature is changed, exhibiting a phase transition. Its phase changes from an insulator (semiconductor) to metallic state when the temperature increases above a value typically near 340K (Liu, 2012). By using different deposition techniques, VO_2 films have been grown on sapphire, quartz, silicon, etc. (Wang, 2005). Jepsen *et al.* investigated that VO_2 on the sapphire substrate is transparent for THz radiation when the temperature is below the transition temperature and therefore it is in the insulator state. However, for nominally high temperatures such as above the transition temperature, VO_2 on the sapphire substrate reflects the THz radiation since it is in the metallic state.

In this study, by using a home-built THz-TDS system, the transmission of the THz radiation was investigated for grown thin films of Vanadium dioxide (VO_2) on different dielectric substrates at different temperatures. After detection of the metal-insulating transition point, grown films were etched and patterned in order to investigate the frequency selective nature of the surface.

2 MEASUREMENTS

2.1 Terahertz Time Domain Spectroscopy

Vanadium dioxide (VO_2) patterned and unpatterned films were characterized using a home-built THz-TDS system. The system utilizes a Photoconductive Antenna (PCA) in generation and electro-optic sampling in detection. A femtosecond Ti:Sapphire mode-lock laser source is used in order to generate and detect the THz radiation. The laser has a 75 MHz repetition rate, 16fs pulse width and 800 nm central wavelength. In this system a beam splitter is used in order to split the output beam of the laser into generation and detection arms. Its transmission ratio is 95:5. The THz signal is detected using electro-optic detection through a 2mm thick <110> oriented ZnTe crystal. A balanced photodiode, lock-in amplifier synced to the function generator driving the modulation on the photoconductive antenna and a personal computer are used to record the THz waveforms.

The THz radiation is generated in a commercially obtained PCA which is modulated at 1 kHz and biased at +/-15V. Afterwards the generated

radiation is collected with the aid of a silicon lens, the THz waves are then collimated by an off-axis parabolic mirror. Then, by using a converging TPX lens, the THz radiation is focused on to the sample in order to have efficient sample-THz interaction. Next, another TPX lens is used in order to collimate the diverging THz beam. Then, by using another off axis parabolic mirror, this beam is collected and focused through onto the ZnTe crystal.
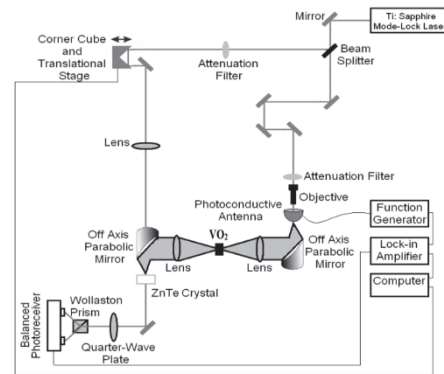

Figure 1: Schematic representation of THz-TDS system.

In the detection arm, the beam is directed onto a corner cube on the top of the translational stage which is used to scan the electric field of the THz waveform. The THz waveform is collected by stepping the stage through the waveform. The femtosecond visible pulse polarization changes as it passes though the electro-optic set-up for different values of the THz electric field. The entire system is controlled using LabView software.

2.2 Closed Cycle Cryostat

In order to control the temperature during the THz measurements a closed cycle cryostat was used which was already in place to perform low temperature measurements on different samples. The system was used in heating mode only and in order to increase and control the temperature starting from room temperature to higher temperatures a temperature controller is used. This system consists of Sumitomo CH-204SFF coldhead and Vacuubrand RZ14 vacuum pump. At the end of the cold head there is a sample holder and sample is mounted there. Also, THz radiation is transmitted through the sample after passing through quartz windows placed around the cold head.

2.3 VO₂

In this study the measurements were done for three samples: unpatterned VO$_2$ on the sapphire substrate, cross shape patterned VO$_2$ on the top of both sapphire and fused silica substrates.

VO$_2$ thin films with a thickness of ~250 nm were deposited on c-cut sapphire (500 μm thick) and fused silica (900 μm thick) substrates by dc magnetron sputtering in 98.5% Ar + 1.5% O$_2$ environment. 2" high purity (99.95%) vanadium (V) was used as sputtering target. VO$_2$ films were fabricated under the same growth conditions for both sapphire and fused silica substrates. Before the substrates were placed into vacuum chamber, these substrates were ultrasonically cleaned in acetone, methanol and propanol for 10 min, respectively. Then, the substrates were dried with pure nitrogen flow. The base pressure in sputtering chamber was below 1.6x10^{-6} Torr, and deposition pressure in the chamber was 8.3x10^{-3} Torr. To remove contaminations from the surface of V target, 10 min pre-sputtering was carried out. Dc power of 50 W was applied to V target. Substrates were heated up to 550 ^{o}C, and this substrate temperature was kept constant during deposition. In addition, in order to improve homogeneity on the film surface, each substrate was rotated at 15 rpm.

To understand the quality of the grown films, the critical temperature and conductive properties of unpatterned VO$_2$ was initially analyzed by using THz-TDS system with the closed cycle cryostat shown above.
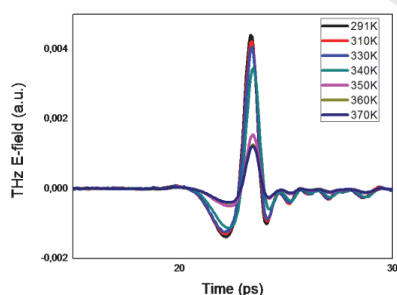

Figure 2: THz E-field vs. time graph for unpatterned 250nm thick VO$_2$ film on sapphire substrate.

In Figure 2 it can be noticed that when VO$_2$ changes between the insulating and the metallic state, amplitude of the electric field of the transmitted wave varies significantly. In Figure 3 this change is shown with respect to frequency after applying a Fourier transform on the time-dependent waveforms. The oscillations are due to the etalon effect which becomes more prominent with increase

of temperature. This is more evident when the critical temperature of the VO$_2$ sample is above 340K. Moreover, it can be said that when the temperature is below the critical temperature the sample is an insulator and when the temperature is above the critical temperature the sample is metallic and there it reflects the THz radiation adding to the observed dips in the etalon. Also, in Figure 4, the THz electric field peak to peak value is plotted with respect to temperature, showing this transition clearly. Therefore, these results are in agreement with the works published previously (Jepsen, 2006). After confirming the critical temperature of VO$_2$, similar films grown on fused silica and sapphire substrates were patterned to investigate the frequency selectivity of the films under changing temperature.
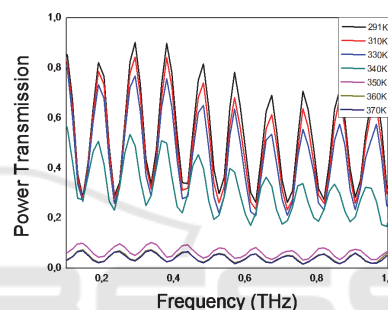

Figure 3: Power transmission vs. frequency graph for unpatterned 250nm thick VO$_2$ film on sapphire substrate.
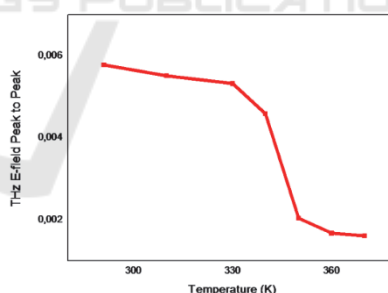

Figure 4: THz E-field peak to peak with respect to temperature for unpatterned 250nm thick VO$_2$ film on sapphire substrate.

2.4 Frequency Selective Surfaces

In this study, a cross shape (Demirhan, 2016) pattern was investigated for VO$_2$ films on sapphire and fused silica substrates. The cross shape patterns were obtained by employing photolithography, and ion beam etching techniques. In Figure 5, the dimensions of the cross shape patterned VO$_2$ on dielectric substrate can be seen.
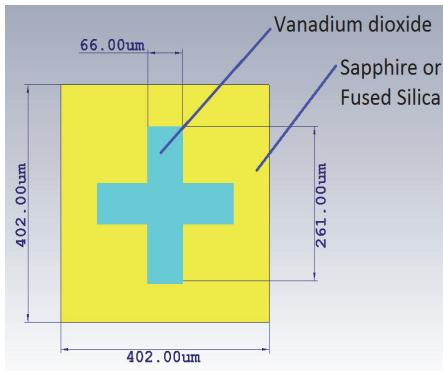
Figure 5: Front view and dimensions of the cross shaped VO₂ unit cell.

Moreover in Figure 6 and Figure 7 the optical microscope images of cross shape patterned VO₂ on sapphire and fused silica substrates is shown.
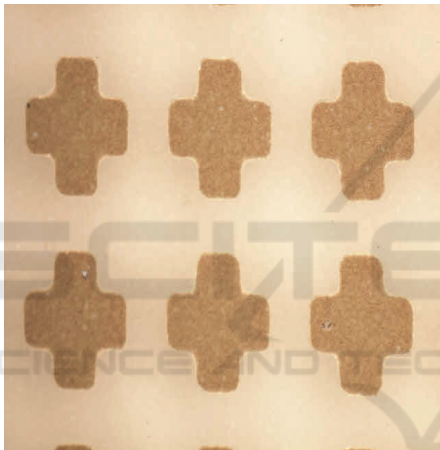

Figure 6: Optical microscope image of 250nm thick VO₂ frequency selective surface on sapphire substrate. The dark areas are VO₂.
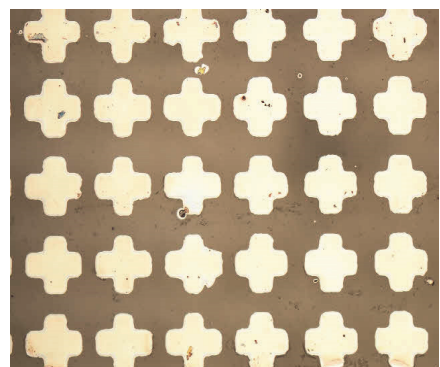

Figure 7: Optical microscope image of 250nm thick VO₂ frequency selective surface on fused silica substrate. The dark areas are VO₂.

3 RESULTS

3.1 Cross Shaped VO₂ on Sapphire Substrate

First, the cross shaped VO₂ on the sapphire substrate is measured using the THz TDS system. In Figure 8 the THz electric field with respect to time can be seen. In Figure 9 the power transmission with respect to the frequency is shown. In this figure the transmission at 299K (initial temperature) was referenced to the transmission at different temperatures.
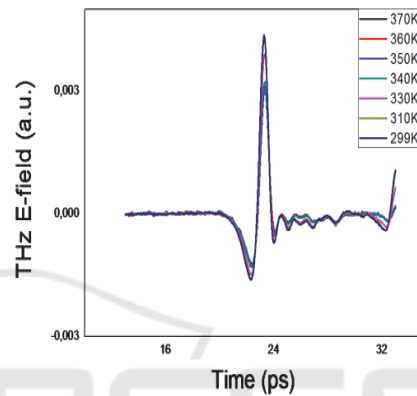

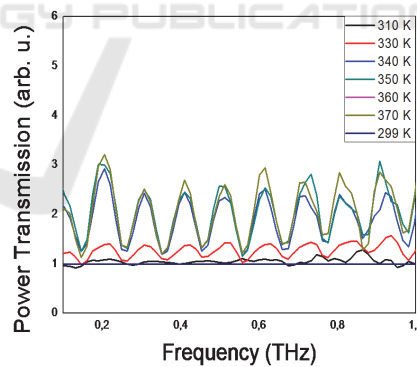Figure 8: THz E-field vs. time graph for cross shape patterned VO₂ for sapphire substrate.

Figure 9: Power transmission with respect to frequency for cross shape patterned VO₂ on sapphire substrate.

3.2 Cross Shaped VO₂ on Fused Silica Substrate

Second, the cross shaped VO₂ on the fused silica substrate is measured using the THz TDS system. The THz electric field with respect to time and power transmission with respect to frequency can be seen in Figure 10 and 11, respectively. In Figure 11 the transmission at 299K (initial temperature) is

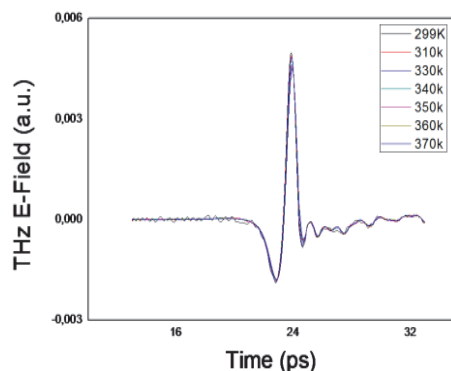referenced to the transmission at different temperatures.

Figure 10: THz E-field vs. time graph for cross shape patterned VO_2 on fused silica substrate.
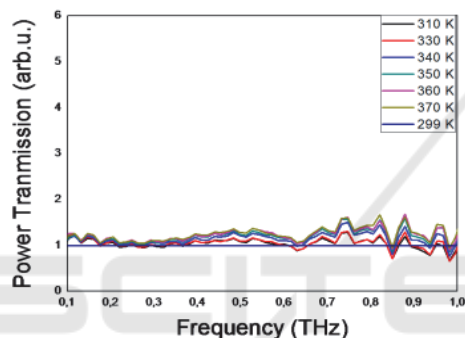

Figure 11: Power transmission vs. frequency graph for cross shape patterned VO_2 on fused silica substrate.

3.3 Analysis

The critical temperature of unpatterned VO_2 is found to be approximately at 340K. This is also evident in the behaviour of the electric field of the incoming THz wave which varies significantly near here. In addition, the unpatterned VO_2 sample is in the metallic state when the temperature is above the critical temperature, and it reflects the THz radiation. Similarly, below the critical temperature, sample is in the insulating state and it is more transparent to the incoming THz radiation.

For the patterned samples, examining Figure 9 the sample is in a more metallic state as the temperature is increased and interestingly enough in this state etalon effects can be observed which also becomes prominent with increase in temperature. In contrast, for the patterned cross shape VO_2 on fused silica substrate (Figure 11) the etalon effects are not apparent. In Figure 8 and Figure 10 both power transmissions are normalized to transmission at higher temperatures. Hence the ratio is expected to

be greater than 1 since the 299K state is more transparent.

The etalon effect in Figure 8 can be analysed to understand the thickness or refractive index of the substrate. The refractive index of sapphire substrate at different temperatures can be calculated using;

$$\Delta f = c/2nd \qquad (1)$$

In this formula c is the speed of light in mm and d is the thickness of sapphire substrate and it is equal to 0.5 mm. The peak difference of the frequency value can be calculated by using Figure 9, this value is measured as 0.103 THz. The calculated real refractive indices for different temperatures are shown in Table 1.

Table 1: Calculated Real Refractive index of sapphire at different temperatures.

Temperature (K)	Refractive index
310	2,93
330	2,93
340	2,93
350	2,93
360	2,93
370	2,93

This table shows that refractive index of sapphire does not change when the temperature is increased and according to this calculation its refractive index is approximately 2.93. Previous measurements have shown that the refractive index of sapphire is nearly 3.00 (Lee, 2009).

In cross shaped VO_2 on fused silica substrate, the etalon effects are not apparent. The thickness of the fused silica substrate is greater than the sapphire substrate and also refractive index of fused silica is smaller than the refractive index of sapphire substrate. Therefore, etalon effects are not seen in fused silica substrate. To explain this, one can examine the difference in refractive index. Refractive of sapphire is approximately 3 and

refractive index of fused silica is approximately 2 (Lee, 2009). Therefore when we compare percentage of power reflection from one interface between these substrates, in sapphire it is ~%25 and in fused silica it is ~%11. In order to see etalon effect, there should be interference and in fused silica this is lower than that of the sapphire substrate as one interface becomes more metallic.

4 CONCLUSION

In this study the transmission of THz radiation is investigated through patterned and unpatterns films of VO_2 grown on dielectric substrates using THz-TDS. The critical temperature for a VO_2 film thickness of 250nm on sapphire substrate is observed to be close to the accepted value of 340K. Above this critical temperature unpatterned VO_2 is in the metallic state and it reflects THz radiation. However, below the critical temperature, unpatterned VO_2 is in the insulating state and it is transparent for THz radiation. After patterning the films deposited on both fused silica and sapphire substrates using a well-known cross shape frequency selective surface pattern the experiments were repeated to observe the frequency selectivity of the devices. Due to the small change in conductivity between insulator and metallic states the frequency selective properties of the patterned VO_2 surface was not observed as was expected if the surface was a pure metallic conductor. While frequency selectivity was not observed, the change in conductivity with temperature was enough to result in an etalon effect which became more evident with increasing temperature for the sapphire substrate sample and not the fused silica substrate sample. The preliminary analysis indicates that the observation of this etalon effect in the sapphire case and not the fused silica case is most likely due to the difference in refractive index between the two substrates. While one surface reflects more for one substrate the other surface becomes equally more metallic as the temperatures increases for both substrate samples.

Future studies will focus on increasing the quality of the VO_2 deposited samples and understanding why any resonance was not observed. The frequency selective nature of the surface failed due most likely to the low conductivity of the film. Previous studies done by our group show that low conductivity in metallic films can result in a decrease in the observed resonance expected with frequency selective surfaces (Demirhan, 2016). Using a commercial software such as CST

Microwave Studio further work will focus on simulating the transmission of the THz pulse through the VO_2 patterned film on both dielectric substrates.

ACKNOWLEDGMENTS

REFERENCES

X. C. Zhang, and J. Xu 2010. "Introduction to THz Wave Photonics" *Springer Science+Business Media, LLC.*

Y. S. Lee 2009. " Principles of Terahertz Science and Technology" Springer Science+Business Media, LLC.

D. Grischkowsky, S. Keiding, M. Exter and C. Fattinger 1990. J. Opt. Am. B/Vol.7 No.10/October 1990

C. L. Holloway, M. A. Mohamed, E. F. Kuester, and A. Dienstfrey 2005. IEEE Transcations on Electromagnetic Compatibility, 47(4):853-865, Nov 2005.

H. T. Chen, W. J. Padilla, J. M. O. Zide, A. C. Gossard, A. J. Taylor, R. D. Averitt 2006. Nature 444,597-600.

P. U. Jepsen, B. M. Fischer, A. Thoman, H. Helm, J. Y. Suh, R. Lopez and R. F. Haglund 2006. Phys. Rev B **74**, 205103.

M. Liu, H. Y. Hwang, H. Tao, A. C. Strikwerda, K. Fan, G. R. Keiser, A. J. Sternbach, K. G. West, S. Kittiwatanakul, J. Lu, S. A. Wolf, F. G. Omenetto, X. Zhang, K. A. Nelson and R. D. Averitt 2012. Nature 487. doi:10.1038/nature11231.

H. Wang, X. Yi, S. Chen, X. Fu 2005. Sensors and Actuators A 122 (2005) 108-112.

Y. Demirhan, H. Alaboz, L. Ozyuzer, M. A. Nebioglu, T. Takan, H. Altan, C. Sabah 2016. Optical and Quantum Electronics, 48(2):1-11.